PRAMANA
— journal of
physics

Vol. 71, No. 1
July 2008
pp. 23–32

Anomalous absorption in H_2CN and CH_2CN molecules

S CHANDRA and S V SHINDE*
School of Physical Sciences, S.R.T.M. University, Nanded 431 606, India
*Corresponding author. E-mail: shivprasad_shinde@yahoo.co.in

MS received 6 November 2007; revised 3 March 2008; accepted 12 March 2008

Abstract. Structures of H_2CN and CH_2CN molecules are similar to that of H_2CO molecule. The H_2CO has shown anomalous absorption for its transition $1_{11} - 1_{10}$ at 4.8 GHz in a number of cool molecular clouds. Though the molecules H_2CN and CH_2CN have been identified in TMC-1 and Sgr B2 through some transitions in ortho as well as in para species, here we have investigated the condition under which transitions $1_{11} - 1_{10}$ and $2_{12} - 2_{11}$ of these molecules may show anomalous absorption.

For the present investigation, we have calculated energy levels and radiative transition probabilities. However, we have used scaled values for collisional rate coefficients. We found that relative values of collisional rate coefficients can produce the required anomalous absorption in $1_{11} - 1_{10}$ and $2_{12} - 2_{11}$ transitions in the molecules.

Keywords. Interstellar molecules; H_2CN; CH_2CN.

PACS Nos 95.30.Ky; 95.30.Jx

1. Introduction

Many radicals, molecular ions and other molecules which have short lifetimes in laboratories are found in many molecular clouds, as well as in the envelopes around evolved stars. Radio astronomers have discovered many molecular lines from the interstellar clouds. Interstellar clouds are neither uniform nor dynamically quiescent on long time-scales. The detailed investigation of the interstellar molecular clouds will give insight into the physical and chemical conditions of these objects. The physical conditions in the interstellar medium are rather extreme as compared to those in the laboratories. The densities are very low, typical values range from 1 to 10^5 particles per cm^{-3} and the temperature ranges from 5 to 60 K in cool molecular clouds such as taurus molecular cloud-1 (TMC-1) and up to several hundred Kelvins in the hot cores of Sagittarius B2 (Sgr B2).

H_2CN (methylene amidogen) is an *a*-type asymmetric top planar molecule having an electric dipole moment of 2.52 D [1]. Ohishi *et al* [2] reported detection of H_2CN molecule through its transition $1_{01} - 0_{00}$ in TMC-1 and transition $2_{02} - 1_{01}$ in Sgr B2. These transitions belong to the para species of the molecule. H_2CN has

a fractional abundance relative to H_2 of $\sim 1.5\times10^{-11}$ [2]. CH_2CN (cyanomethyl radical) is also an *a*-type asymmetric top planar molecule having an electric dipole moment of 1.621 D [3]. Irvine *et al* [4] reported detection of CH_2CN in TMC-1 and Sgr B2 through its transitions $1_{01}-0_{00}$, $2_{02}-1_{01}$, $2_{12}-1_{11}$, $4_{04}-3_{03}$, $5_{05}-4_{04}$ and $5_{14}-4_{13}$. Here, the transitions belong to both ortho as well as para species. CH_2CN has a fractional abundance relative to H_2 of $\sim 5\times10^{-9}$ [4].

The anomalous absorption was first detected for the transition $1_{11}-1_{10}$ in H_2CO molecule [5]. Here, we are interested to find out the condition under which the transition $1_{11}-1_{10}$ of H_2CN as well as CH_2CN molecules can be found in anomalous absorption. With the calculated radiative transition probabilities and scaled values of collisional rates, we have solved a set of statistical equilibrium equations coupled with the equations of radiative transfer. Following the information about collisional rates for H_2CO molecule, we modified the collisional rates for some transitions and found that the transitions $1_{11}-1_{10}$ and $2_{12}-2_{11}$ of the present molecules can also be found in anomalous absorption.

We propose identification of H_2CN molecule through its transitions $1_{11}-1_{10}$ and $2_{12}-2_{11}$ at 4.92 and 14.72 GHz, respectively and of CH_2CN molecule through the same transitions at 2.19 and 1.11 GHz, respectively, and through absorption against the cosmic microwave background (CMB). In the investigation, relative values of collisional rate coefficients are found to play an important role in the mechanism of anomalous absorption.

2. Modeling

We have calculated rotational energy levels (table 1) by using the molecular and distortional constants for H_2CN [6] and for CH_2CN [7]. The lines of our interest, $1_{11}-1_{10}$ and $2_{12}-2_{11}$ belong to the ortho species of both molecules. In the investigation, we have solved a set of 30 simultaneous equations coupled with 66 equations of radiative transfer for H_2CN molecule. For CH_2CN molecule, a set of 20 simultaneous equations coupled with 28 equations of radiative transfer are solved. The statistical equilibrium equations coupled with equations of radiative transfer can be expressed as follows:

$$n_i \sum_{\substack{j=1\\ j\neq i}}^{z} P_{ij} = \sum_{\substack{j=1\\ j\neq i}}^{z} n_j P_{ji}, \quad i = 1, 2, \ldots, z,$$

where $z = 30$ for H_2CN and $z = 20$ for CH_2CN. Here, n's are the population densities of the rotational levels and the parameter P is:

(i) For optically allowed transitions,

$$P_{ij} = \begin{cases} (A_{ij} + B_{ij} I_{\nu,bg})\beta_{ij} + n_{\mathrm{H_2}} C_{ij}, & i > j \\ B_{ij} I_{\nu,bg} \beta_{ij} + n_{\mathrm{H_2}} C_{ij}, & i < j \end{cases}.$$

(ii) For optically forbidden transitions,

Table 1. Energies (in cm^{-1}) of rotational levels of ortho species of H_2CN and CH_2CN.

H_2CN					
$J_{k_a k_c}$	Energy	$J_{k_a k_c}$	Energy	$J_{k_a k_c}$	Energy
1_{11}	10.627	6_{16}	57.918	5_{33}	111.111
1_{10}	10.791	6_{15}	61.351	5_{32}	111.112
2_{12}	15.360	7_{17}	74.450	9_{19}	114.559
2_{11}	15.851	7_{16}	79.025	9_{18}	121.895
3_{13}	22.458	3_{31}	89.077	6_{34}	125.804
3_{12}	23.440	3_{30}	89.077	6_{33}	125.805
4_{14}	31.919	8_{18}	93.332	$10_{1,10}$	138.127
4_{13}	33.555	4_{32}	98.869	7_{35}	142.948
5_{15}	43.740	4_{31}	98.870	7_{34}	142.952
5_{14}	46.193	8_{17}	99.208	10_{19}	147.078
CH_2CN					
$J_{k_a k_c}$	Energy	$J_{k_a k_c}$	Energy	$J_{k_a k_c}$	Energy
1_{11}	9.860	4_{13}	15.969	8_{18}	33.135
1_{10}	9.873	5_{15}	19.171	8_{17}	33.579
2_{12}	11.190	5_{14}	19.356	9_{19}	39.127
2_{11}	11.227	6_{16}	23.161	9_{18}	39.675
3_{13}	13.185	6_{15}	23.419	$10_{1,10}$	45.769
3_{12}	13.259	7_{17}	27.815	10_{19}	46.449
4_{14}	15.846	7_{16}	28.161		

$$P_{ij} = n_{\mathrm{H_2}} C_{ij},$$

where A's and B's are Einstein coefficients,

$$A_{ul} = \frac{2h\nu^3}{c^2} B_{ul}, \quad B_{ul} = \frac{g_l}{g_u} B_{lu},$$

where C's are the collisional rate coefficients, $n_{\mathrm{H_2}}$ is the density of hydrogen molecules, and the escape probability β for the transition is

$$\beta_{lu} = \beta_{ul} = \frac{1 - \exp(-\tau_\nu)}{\tau_\nu},$$

where optical thickness τ_ν is

$$\tau_\nu = \frac{hc}{4\pi(\mathrm{d}v_\mathrm{r}/\mathrm{d}r)}[B_{lu} n_l - B_{ul} n_u].$$

Here, $(\mathrm{d}v_\mathrm{r}/\mathrm{d}r)$ is the velocity gradient in the region. By solving these coupled equations, population densities of the levels are calculated. This set of equations is solved through iterative procedure for the given values of $n_{\mathrm{H_2}}$ and $\gamma \equiv n_{\mathrm{mol}}/(\mathrm{d}v_\mathrm{r}/\mathrm{d}r)$,

Table 2. Einstein A-coefficients of H_2CN and CH_2CN molecules.

H_2CN					
Transition	A-coeff. (s^{-1})	Transition	A-coeff. (s^{-1})	Transition	A-coeff. (s^{-1})
$1_{10} \rightarrow 1_{11}$	4.363×10^{-9}	$2_{12} \rightarrow 1_{11}$	6.334×10^{-5}	$2_{11} \rightarrow 1_{10}$	7.741×10^{-5}
$2_{11} \rightarrow 2_{12}$	3.926×10^{-8}	$3_{13} \rightarrow 2_{12}$	2.713×10^{-4}	$3_{12} \rightarrow 2_{11}$	3.315×10^{-4}
$3_{12} \rightarrow 3_{13}$	1.570×10^{-7}	$4_{14} \rightarrow 3_{13}$	7.026×10^{-4}	$4_{13} \rightarrow 3_{12}$	8.587×10^{-4}
$4_{13} \rightarrow 4_{14}$	4.361×10^{-7}	$5_{15} \rightarrow 4_{14}$	1.435×10^{-3}	$5_{14} \rightarrow 4_{13}$	1.754×10^{-3}
$5_{14} \rightarrow 5_{15}$	9.811×10^{-7}	$6_{16} \rightarrow 5_{15}$	2.547×10^{-3}	$6_{15} \rightarrow 5_{14}$	3.112×10^{-3}
$6_{15} \rightarrow 6_{16}$	1.923×10^{-6}	$7_{17} \rightarrow 6_{16}$	4.113×10^{-3}	$7_{16} \rightarrow 6_{15}$	5.025×10^{-3}
$7_{16} \rightarrow 7_{17}$	3.418×10^{-6}	$3_{31} \rightarrow 2_{12}$	6.906×10^{-6}	$3_{31} \rightarrow 3_{12}$	4.459×10^{-6}
$3_{31} \rightarrow 4_{14}$	6.993×10^{-7}	$3_{30} \rightarrow 2_{11}$	6.973×10^{-6}	$3_{30} \rightarrow 3_{13}$	4.393×10^{-6}
$3_{30} \rightarrow 4_{13}$	7.078×10^{-7}	$8_{18} \rightarrow 7_{17}$	6.209×10^{-3}	$4_{32} \rightarrow 3_{13}$	1.547×10^{-5}
$4_{32} \rightarrow 4_{13}$	1.129×10^{-5}	$4_{32} \rightarrow 5_{15}$	1.776×10^{-6}	$4_{32} \rightarrow 3_{31}$	3.636×10^{-4}
$4_{31} \rightarrow 3_{12}$	1.579×10^{-5}	$4_{31} \rightarrow 4_{14}$	1.101×10^{-5}	$4_{31} \rightarrow 5_{14}$	1.798×10^{-6}
$4_{31} \rightarrow 3_{30}$	3.636×10^{-4}	$8_{17} \rightarrow 7_{16}$	7.583×10^{-3}	$8_{17} \rightarrow 8_{18}$	5.652×10^{-6}
$5_{33} \rightarrow 4_{14}$	2.651×10^{-5}	$5_{33} \rightarrow 5_{14}$	2.018×10^{-5}	$5_{33} \rightarrow 6_{16}$	3.013×10^{-6}
$5_{33} \rightarrow 4_{32}$	1.063×10^{-3}	$5_{32} \rightarrow 4_{13}$	2.749×10^{-5}	$5_{32} \rightarrow 5_{15}$	1.944×10^{-5}
$5_{32} \rightarrow 6_{15}$	3.037×10^{-6}	$5_{32} \rightarrow 4_{31}$	1.063×10^{-3}	$9_{19} \rightarrow 8_{18}$	8.909×10^{-3}
$9_{18} \rightarrow 8_{17}$	1.088×10^{-2}	$9_{18} \rightarrow 9_{19}$	8.836×10^{-6}	$6_{34} \rightarrow 5_{15}$	4.055×10^{-5}
$6_{34} \rightarrow 6_{15}$	3.109×10^{-5}	$6_{34} \rightarrow 7_{17}$	4.267×10^{-6}	$6_{34} \rightarrow 5_{33}$	2.186×10^{-3}
$6_{33} \rightarrow 5_{14}$	4.296×10^{-5}	$6_{33} \rightarrow 6_{16}$	2.950×10^{-5}	$6_{33} \rightarrow 7_{16}$	4.255×10^{-6}
$6_{33} \rightarrow 5_{32}$	2.187×10^{-3}	$10_{1,10} \rightarrow 9_{19}$	1.229×10^{-2}	$7_{35} \rightarrow 6_{16}$	5.802×10^{-5}
$7_{35} \rightarrow 7_{16}$	4.405×10^{-5}	$7_{35} \rightarrow 8_{18}$	5.440×10^{-6}	$7_{35} \rightarrow 6_{34}$	3.823×10^{-3}
$7_{34} \rightarrow 6_{15}$	6.312×10^{-5}	$7_{34} \rightarrow 7_{17}$	4.106×10^{-5}	$7_{34} \rightarrow 8_{17}$	5.320×10^{-6}
$7_{34} \rightarrow 6_{33}$	3.825×10^{-3}	$10_{19} \rightarrow 9_{18}$	1.499×10^{-2}	$10_{19} \rightarrow 10_{1,10}$	1.321×10^{-5}
CH_2CN					
$1_{10} \rightarrow 1_{11}$	7.7269×10^{-13}	$2_{12} \rightarrow 1_{11}$	5.8179×10^{-7}	$2_{11} \rightarrow 1_{10}$	6.147×10^{-7}
$2_{11} \rightarrow 2_{12}$	6.9530×10^{-12}	$3_{13} \rightarrow 2_{12}$	2.4930×10^{-6}	$3_{12} \rightarrow 2_{11}$	2.634×10^{-6}
$3_{12} \rightarrow 3_{13}$	2.7810×10^{-11}	$4_{14} \rightarrow 3_{13}$	6.4630×10^{-6}	$4_{13} \rightarrow 3_{12}$	6.829×10^{-6}
$4_{13} \rightarrow 4_{14}$	7.7250×10^{-11}	$5_{15} \rightarrow 4_{14}$	1.3220×10^{-5}	$5_{14} \rightarrow 4_{13}$	1.397×10^{-5}
$5_{14} \rightarrow 5_{15}$	1.7380×10^{-10}	$6_{16} \rightarrow 5_{15}$	2.3490×10^{-5}	$6_{15} \rightarrow 5_{14}$	2.482×10^{-5}
$6_{15} \rightarrow 6_{16}$	3.4060×10^{-10}	$7_{17} \rightarrow 6_{16}$	3.8000×10^{-5}	$7_{16} \rightarrow 6_{15}$	4.015×10^{-5}
$7_{16} \rightarrow 7_{17}$	6.0550×10^{-10}	$8_{18} \rightarrow 7_{17}$	5.7470×10^{-5}	$8_{17} \rightarrow 7_{16}$	6.072×10^{-5}
$8_{17} \rightarrow 8_{18}$	1.0010×10^{-9}	$9_{19} \rightarrow 8_{18}$	8.2910×10^{-5}	$9_{18} \rightarrow 8_{17}$	8.731×10^{-5}
$9_{18} \rightarrow 9_{19}$	1.5050×10^{-9}	$10_{1,10} \rightarrow 9_{19}$	1.1390×10^{-4}	$10_{19} \rightarrow 9_{18}$	1.208×10^{-4}
$10_{19} \rightarrow 10_{1,10}$	2.3510×10^{-9}				

where n_{mol} is the density of the molecule and $(\mathrm{d}v_{\mathrm{r}}/\mathrm{d}r)$ is the velocity gradient in the region. In our investigation, non-local thermal equilibrium (NLTE) occupation numbers of the energy levels are calculated in an on-the-spot approximation by using the escape probability method [8], where the external radiation field, impinging on the volume element generating lines, is the CMB only.

The input data required in the investigation are the radiative transition probabilities (Einstein A-coefficients) and the collisional rate coefficients.

3. Einstein *A*-coefficients

Both H_2CN and CH_2CN are *a*-type asymmetric top molecules and the rotational radiative transitions are governed by the selection rules:

$$\begin{aligned} J \quad &: \Delta J = 0, \pm 1 \\ k_a, k_c \; &: \text{even, odd} \longleftrightarrow \text{even, even} \\ &\quad \text{odd, even} \longleftrightarrow \text{odd, odd,} \end{aligned}$$

where J is the rotational quantum number and k_a and k_c are projections of J on the axis of symmetry in case of prolate and oblate symmetric tops, respectively. In the representation, where the axis of quantization is along the *a*-axis of inertia, Einstein *A*-coefficient for the transition $J'_{\tau'} \rightarrow J_\tau$ is given by [9,10]

$$A(J'_{\tau'} \rightarrow J_\tau) = \frac{64\pi^4\nu^3\mu^2(2J+1)}{3hc^3(2J'+1)} \left[\sum_{K=-J}^{J} g^J_{\tau K} g^{J'}_{\tau' K} C^{J'K}_{JK10} \right]^2, \tag{1}$$

where μ is the electric dipole moment of the molecule, $\mathbf{C}^{\cdot\cdot}_{\cdot\cdot\cdot\cdot}$ the Clebsch Gordon coefficient and $\tau = k_a - k_c$ is a pseudoquantum number. Einstein *A*-coefficients for 66 radiative transitions between 30 energy levels of H_2CN and for 28 radiative transitions between 20 energy levels of CH_2CN are calculated. The values of *A*-coefficients are given in table 2.

4. Collisional rate coefficients

The collisional rate coefficients for H_2CN and CH_2CN are not available in literature and therefore, we have used scaled values for them. The rate coefficients for downward transitions $J'_{k'_a k'_c} \rightarrow J_{k_a k_c}$ at kinetic temperature T_k are taken as [11]

$$C(J'_{k'_a k'_c} \rightarrow J_{k_a k_c}) = 1 \times 10^{-11}\ (2J+1)\sqrt{\frac{T_\mathrm{k}}{30}}. \tag{2}$$

This relation for collisional rate coefficients can be interpreted as cross-section times the thermal velocity. For the upward collisional rate coefficients, we accounted for the fact that downward and upward collisional rate coefficients are related through the detailed equilibrium [12]

$$C(J_{k_a k_c} \rightarrow J'_{k'_a k'_c}) = C(J'_{k'_a k'_c} \rightarrow J_{k_a k_c})\ \frac{2J'+1}{2J+1}\ \exp\left(-\frac{\Delta E}{kT_\mathrm{k}}\right), \tag{3}$$

where ΔE is the energy difference between the corresponding levels. In the absence of accurate collisional rates, our results can be treated as qualitative in nature.

5. Anomalous absorption

Temperature of the CMB (2.73 K) is supposed to be the minimum in the Universe. Thus, no radiation from any cosmic object are supposed to show absorption against

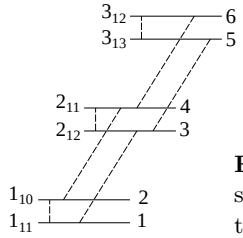

Figure 1. A set of three consecutive doublets corresponding to $J = 1, 2$ and 3 levels along with the radiative transitions between them.

the cosmic microwave background. The observation of a spectral line in absorption against the CMB is an unusual phenomenon, called as the anomalous absorption. The intensity, I_ν, of a line generated with homogeneous excitation conditions, is given by

$$I_\nu - I_{\nu,\mathrm{bg}} = (S_\nu - I_{\nu,\mathrm{bg}})(1 - \mathrm{e}^{-\tau_\nu}), \tag{4}$$

where $I_{\nu,\mathrm{bg}}$ is the intensity of the continuum against which the line is observed, τ_ν is the optical depth and S_ν is the source function. In the Rayleigh–Jeans limit, we have [13]

$$T_\mathrm{B} = T_\mathrm{ex} + (T_\mathrm{bg} - T_\mathrm{ex})\mathrm{e}^{-\tau_\nu}. \tag{5}$$

For anomalous absorption, the excitation temperature T_ex, brightness temperature T_B and the background temperature T_bg satisfy the condition $0 < T_\mathrm{ex} < T_\mathrm{B} < T_\mathrm{bg}$.

6. Results and discussion

In our model, free parameters are the molecular hydrogen density n_{H_2} and γ. Ohishi *et al* [2] and Irvine *et al* [4] found column density 10^{14} cm^{-2} for H_2CN and CH_2CN molecules, in Sgr B2 which corresponds to $\gamma = 10^{-5}$ for $\Delta v = 0.33$ km s^{-1}. Therefore, we have taken $\gamma = 10^{-5}$ and 10^{-6} cm^{-3} (km/s)$^{-1}$ pc. In order to include large number of molecular clouds where these molecules may be found, n_{H_2} is varied over a wide range from 10^2 to 10^6 cm^{-3}, and calculations are performed for kinetic temperatures of 10, 20 and 30 K.

All energy levels of these molecules are in the form of doublets. The observed lines in absorption are due to the transitions between the levels of a doublet. In the terminology of Chandra *et al* [13], the levels 1, 2, 3, 4, 5 and 6 are 1_{11}, 1_{10}, 2_{12}, 2_{11}, 3_{13} and 3_{12} respectively, as shown in figure 1.

6.1 *Anomalous absorption in the* $1_{11} - 1_{10}$ *transition*

For anomalous absorption of the transition $1_{11} - 1_{10}$, in the optically thin limit a rough estimate made by Chandra *et al* [13] shows that rate coefficient C_{14} must be smaller than C_{23}. This criterion is similar to that derived by Townes and Cheung [14] semi-classically and by Green *et al* [15] on the basis of quantum mechanical calculations for H_2CO. Equation (2) here gives $C_{14} \approx C_{23}$ and therefore, we reduced

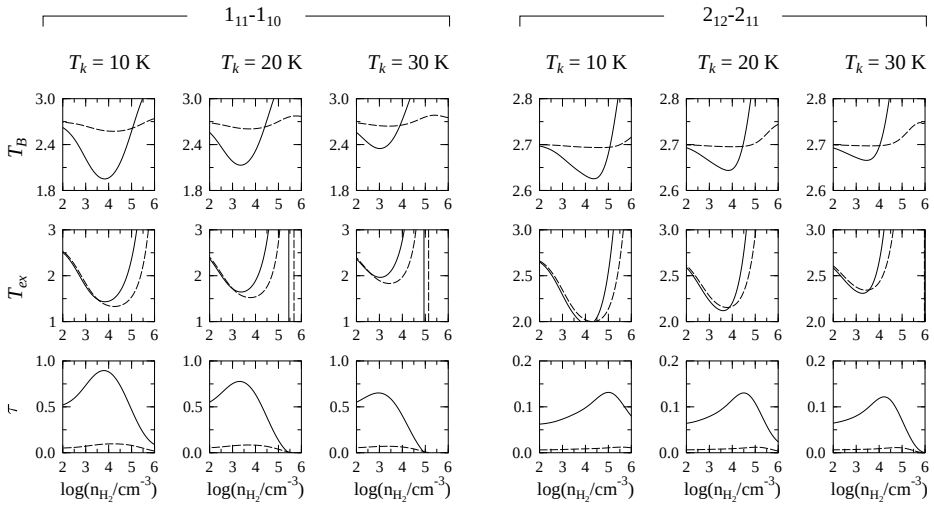

Figure 2. Variation of brightness temperature $T_{\rm B}$ (K), excitation temperature $T_{\rm ex}$ (K) and optical depth τ vs. hydrogen density $n_{\rm H_2}$ of the molecule H_2CN for kinetic temperatures 10, 20 and 30 K. Solid line is for $\gamma = 10^{-5}$ cm^{-3} (km/s)$^{-1}$ pc, and the dotted line for $\gamma = 10^{-6}$ cm^{-3} (km/s)$^{-1}$ pc. Collision rates of the transition $2_{11} - 1_{11}$, and its reverse are reduced by a factor of 2 with respect to that of the calculations from eq. (2).

the rate C_{41} and its reverse by a factor of 2 with respect to that of the calculations from eq. (2). This factor 2 is not very large. By doing so, the transition $1_{11} - 1_{10}$ is found to show the brightness temperature less than 2.73 K for kinetic temperatures 10–30 K (figure 2 for H_2CN and figure 3 for CH_2CN). However, transition $2_{12} - 2_{11}$ shows a weaker anomalous absorption than that of transition $1_{11} - 1_{10}$.

6.2 *Anomalous absorption in the* $2_{12} - 2_{11}$ *transition*

Following the rough estimate made by Chandra *et al* [13], to get anomalous absorption for transition $2_{12} - 2_{11}$, we have reduced the rates C_{41}, C_{42}, C_{61}, C_{62}, C_{63} and their reverse by a factor of 2 with respect to that of the calculations from eq. (2). After reducing the rate coefficients, anomalous absorption in both the transitions $1_{11} - 1_{10}$ and $2_{12} - 2_{11}$ is found to increase (figure 4 for H_2CN and figure 5 for CH_2CN). In both situations anomalous absorption in transition $1_{11} - 1_{10}$ is stronger than that of transition $2_{12} - 2_{11}$. The regions with kinetic temperature around 10 K and molecular hydrogen density around 10^4 cm^{-3} are the best sites for the detection of these molecules through anomalous absorption of $1_{11} - 1_{10}$ and $2_{12} - 2_{11}$ transitions. With the increase of kinetic temperature ($T_{\rm k}$), position of the minimum value of brightness temperature ($T_{\rm B}$) and maximum value of optical depth (τ) are found to shift toward the low density region and the absorption is found to decrease.

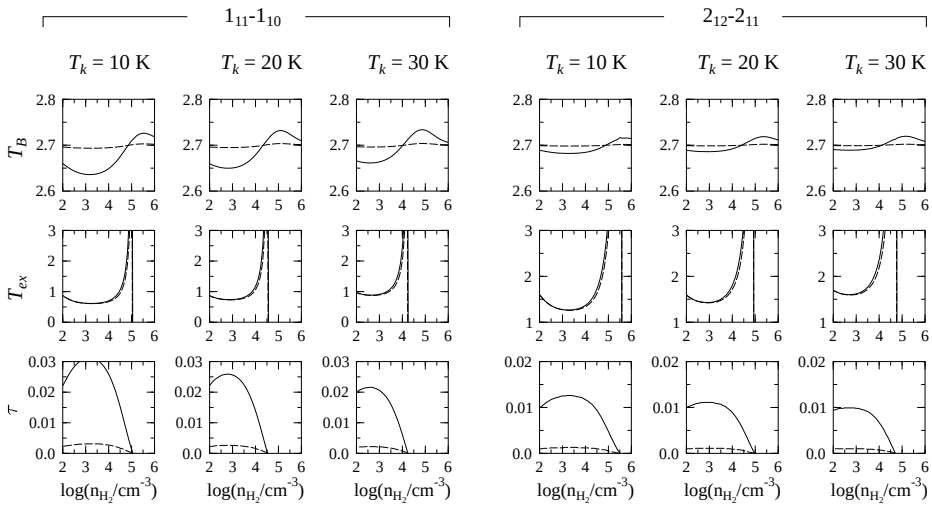

Figure 3. Variation of brightness temperature $T_{\rm B}$ (K), excitation temperature $T_{\rm ex}$ (K) and optical depth τ vs. hydrogen density $n_{\rm H_2}$ of the molecule CH_2CN for kinetic temperatures 10, 20 and 30 K. Solid line is for $\gamma = 10^{-5}$ cm^{-3} (km/s)$^{-1}$ pc, and the dotted line for $\gamma = 10^{-6}$ cm^{-3} (km/s)$^{-1}$ pc. Collision rates of the transition $2_{11} - 1_{11}$, and its reverse are reduced by a factor of 2 with respect to that of the calculations from eq. (2).

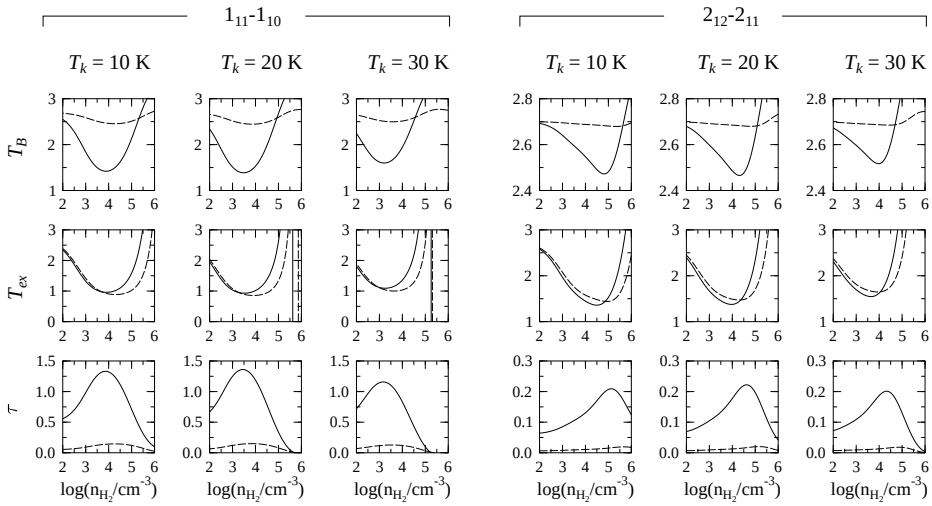

Figure 4. Same as figure 2 but the collision rates of the transitions $2_{11} - 1_{11}$, $3_{12} - 1_{11}$, $3_{12} - 1_{10}$, $3_{12} - 2_{12}$, $2_{11} - 1_{10}$ and their reverse are reduced by a factor of 2 with respect to that of the calculations from eq. (2).

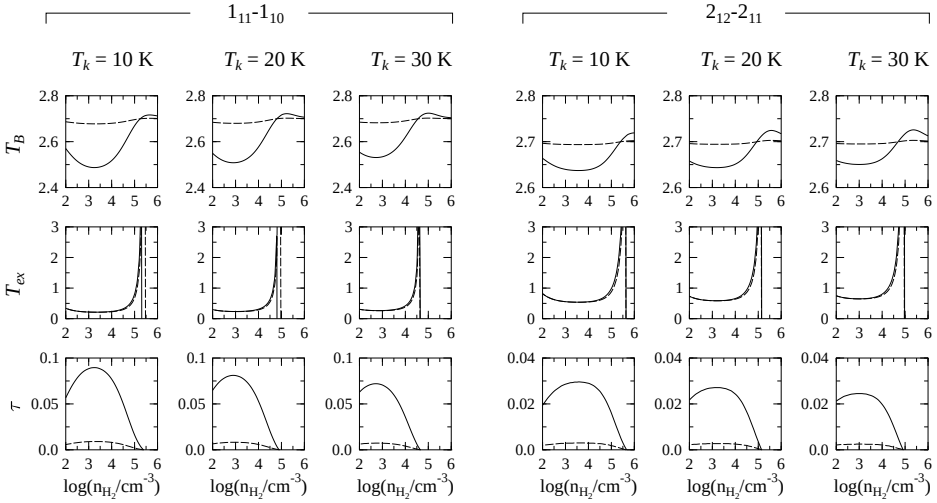

Figure 5. Same as figure 3 but the collision rates of the transitions $2_{11}-1_{11}$, $3_{12}-1_{11}$, $3_{12}-1_{10}$, $3_{12}-2_{12}$, $2_{11}-1_{10}$ and their reverse are reduced by a factor of 2 with respect to that of the calculations from eq. (2).

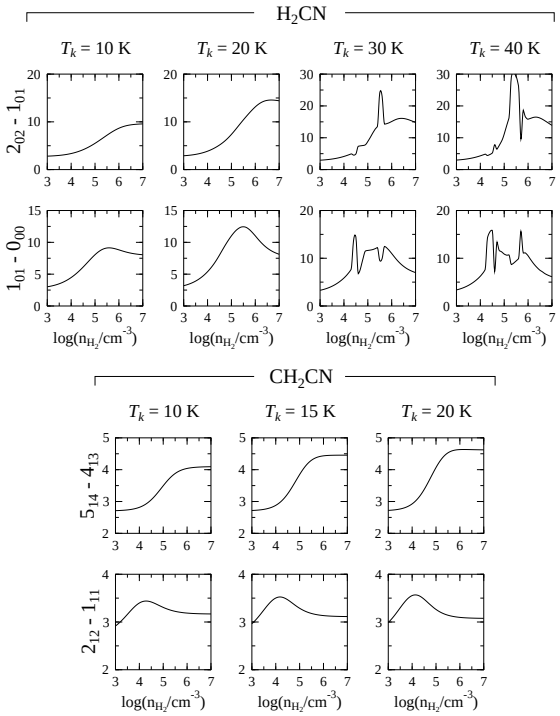

Figure 6. Variation of brightness temperature $T_{\rm B}$ vs. hydrogen density $n_{\rm H_2}$ at different kinetic temperatures and $\gamma = 10^{-5}$ cm^{-3} (km/s)$^{-1}$ pc for observed lines.

We have also calculated the brightness temperature T_B, excitation temperature T_{ex} and optical depth τ for the observed lines $1_{01} - 0_{00}$ and $2_{02} - 1_{01}$ of H_2CN and lines $2_{12} - 1_{11}$ and $5_{14} - 4_{13}$ of CH_2CN. The results confirm the emission feature of these lines. The fluctuation in the brightness temperature for the transitions $1_{01} - 0_{00}$ and $2_{02} - 1_{01}$ for temperatures 30 and 40 K (figure 6) are due to numerical instabilities. In principle, the variation should be smooth.

7. Conclusion

Our investigation shows that H_2CN and CH_2CN may be identified through anomalous absorption of $1_{11} - 1_{10}$ and $2_{12} - 2_{11}$ transitions in the cool cosmic objects. Though these molecules have been identified through emission lines, the anomalous absorption of the said lines can be used for confirmation purposes.

Acknowledgments

We are grateful to Prof. Jayant V Narlikar and Prof. Dr W H Kegel for their encouragement. Thanks are due to the Indian Space Research Organization, Bangalore and the Department of Science and Technology, New Delhi for financial assistance in the form of research projects.

References

[1] D C Cowles, M J Travers, J L Frueh and G B Ellison, *J. Chem. Phys.* **94**, 3517 (1991)
[2] M Ohishi, D McGonagle, W M Irvine, S Yamamoto and S Saito, *Astrophys. J.* **427**, L51 (1994)
[3] A Hinchliffe, *J. Molec. Structure* **53**, 147 (1979)
[4] W M Irvine, P Friberg, A Hjalmarson, S Ishikawa, N Kaifu, K Kawaguchi, S C Madden, H E Matthews, M Ohishi, S Saito, H Suzuki, P Thaddeus, B E Turner, S Yamamoto and L M Ziurys, *Astrophys. J.* **334**, L107 (1988)
[5] P Palmer, B Zuckerman, D Buhl and L E Snyder, *Astrophys. J.* **156**, L147 (1969)
[6] S Yamamoto and S Saito, *J. Chem. Phys.* **96**, 4157 (1992)
[7] S Saito, S Yamamoto, W M Irvine, L M Ziurys, H Suzuki, M Ohishi and N Kaifu, *Astrophys. J.* **334**, L113 (1988)
[8] E Rauch, W H Kegel, T Tusji and G Piehler, *Astron. Astrophys.* **315**, 533 (1988)
[9] S Chandra and A Sahu, *Astron. Astrophys.* **272**, 700 (1993)
[10] S Chandra and Rashmi, *Astron. Astrophys. Suppl.* **131**, 137 (1998)
[11] S Chandra, S V Shinde, W H Kegel and E Sedlmayr, *Astron. Astrophys.* **467**, 371 (2007)
[12] S Chandra, W H Kegel, *Astron. Astrophys. Suppl.* **142**, 113 (2000)
[13] S Chandra, P G Musrif, R M Dharmkare and Monika Sharma, *New Astronomy* **11**, 495 (2006)
[14] C H Townes and A C Cheung, *Astrophys. J.* **157**, L103 (1969)
[15] S Green, B J Garrison, W A Lester Jr. and W H Miller, *Astrophys. J. Suppl.* **37**, 321 (1978)